



**HAL**  
open science

# Carrier Anisotropy and Impurity Scattering in Germanium at mK Temperatures: Modeling and Comparison to Experiment

A. Broniatowski

► **To cite this version:**

A. Broniatowski. Carrier Anisotropy and Impurity Scattering in Germanium at mK Temperatures: Modeling and Comparison to Experiment. 14th International Workshop on Low Temperature Detectors, Aug 2011, Heidelberg, Germany. pp.1069-1074, 10.1007/s10909-012-0543-5 . in2p3-00674793

**HAL Id: in2p3-00674793**

**<https://in2p3.hal.science/in2p3-00674793v1>**

Submitted on 28 Feb 2012

**HAL** is a multi-disciplinary open access archive for the deposit and dissemination of scientific research documents, whether they are published or not. The documents may come from teaching and research institutions in France or abroad, or from public or private research centers.

L'archive ouverte pluridisciplinaire **HAL**, est destinée au dépôt et à la diffusion de documents scientifiques de niveau recherche, publiés ou non, émanant des établissements d'enseignement et de recherche français ou étrangers, des laboratoires publics ou privés.

Proceedings 14<sup>th</sup> International Workshop on Low Temperature Detectors (Heidelberg, Germany, 2011), to appear in Journal of Low Temperature Physics (2012). DOI: 10.1007/s10909-012-0543-5

## **Carrier Anisotropy and Impurity Scattering in Germanium at mK Temperatures: Modeling and Comparison to Experiment**

**A. Broniatowski<sup>(\*)</sup>**

*Centre de Spectrométrie Nucléaire et de Spectrométrie de Masse,  
IN2P3/CNRS and Université Paris XI, Bât. 108, 91405 Orsay (France)*

*Improving upon the present background rejection capabilities of the cryogenic Ge detectors for direct dark matter search involves an in-depth comprehension of the charge collection process in these devices. Experimental data point to the combined effects of lattice and impurity scattering on the anisotropy of electron transport in germanium at mK temperatures. A Monte Carlo simulation code has been implemented to incorporate these features in a consistent model of charge collection. In a novel approach to carrier scattering by charged impurities, the scattering field of the impurities is treated statistically as a random contribution to the collection field, described by the Holtsmark distribution function with a single adjustable parameter, the mean density of the charged centers. Simulation of charge collection along these lines in devices different by their impurity content shows excellent agreement to experiment. Especially noteworthy is the fact that the strength of impurity scattering is reversed from the known concentration of dopant impurities in the crystals, as the crystal with the higher dopant concentration shows lower scattering at low field than the one with the lower concentration. This raises as an issue for further improvement of these devices, the question of the nature of the scattering centers in high-purity Ge crystals at cryogenic temperatures, associated presumably with deep level impurities or crystal defects.*

### **1. INTRODUCTION**

This paper is a follow-up of an experimental study of anisotropy effects in hot carrier transport in germanium at mK temperatures, and their bearing

(\*) corresponding author. e-mail: alexandre.broniatowski@csnsm.in2p3.fr

### A. Broniatowski

on charge collection in cryogenic Ge detectors for dark matter search.<sup>1</sup> The main results of the experimental part summarize as follows:

(i) In the field range typical for the operation of these devices ( $\sim 1$  V/cm), electrons exhibit effects of transport anisotropy on the macroscopic scale, with a transverse straggle comparable to their projected path along the direction of the field. Hole straggle is comparatively on a much smaller scale.

(ii) The scattering processes involved vary depending on the field, with lattice scattering dominant at the larger values of the field ( $> \sim 5$  V/cm), and impurity scattering increasingly important at lower field intensities.

(iii) Impurity effects on electron straggling vary in magnitude depending on the concentration of electrically active centers, which raises the question of the nature and the densities of the impurity or defect centers involved.

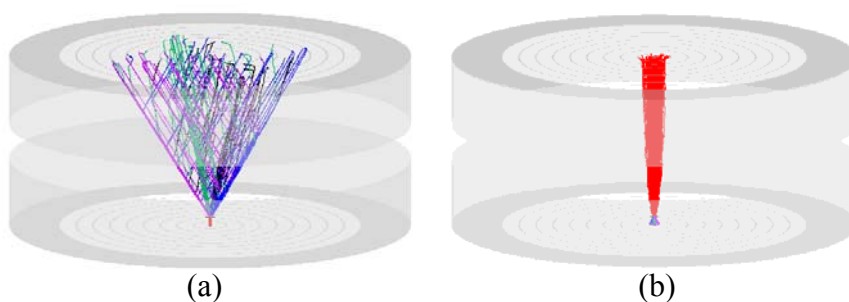


Fig. 1. (a) Simulated carrier trajectories for a 60 keV energy deposit from a collimated  $^{241}\text{Am}$   $\gamma$  source facing the bottom surface of the detector crystal. See ref. 1 for a full description of the device and of the geometry of the charge collection field especially. Detector bias  $V_p = 2$  V;  $T = 20$  mK. Holes are in red and electrons in blue, black, green and magenta depending on their valley of belonging. (b) Same as (a), with the polarity of the electrode biases reversed so that holes instead of electrons are drifted across the full thickness of the detector crystal.

To illustrate these features of electron and hole transport, figure 1 represents the carrier trajectories simulated for an energy deposit near the bottom surface of the detector crystal, for the case that the electrons (a) or the holes (b) are drifted across the full thickness of the device. A comparison of these figures underlines the role of carrier anisotropy in determining the patterns of charge collection. Figure 1 (a) illustrates in particular the importance of intervalley scattering on electron straggle, with the intervalley

## Carrier anisotropy in Ge at mK temperatures: modeling

transitions appearing as the sharp bends in the electron trajectories. Such simulations, in conjunction with the experimental data for electron collection in specimens of different crystal purities,<sup>1</sup> bring to attention the role of impurity scattering in relation to the intervalley transition rates. We analyze this connection in section 2, based on a statistical model for the field fluctuations produced by a random distribution of charged impurities, applicable to the low-temperature range of carrier freeze-out in germanium (below 1 K typically). This model provides the basis for Monte Carlo simulations of electron transport and the charge collection process in the detectors (sec. 3). Section 4 analyses the charge collection patterns obtained by measurements on two devices different by their impurity content. Issues in Ge characterization are discussed in conclusion.

## 2. IMPURITY SCATTERING AND ELECTRON ANISOTROPY

Intervalley scattering by charged and neutral donor impurities in germanium was demonstrated long ago by studies of the acoustoelectric effect,<sup>2</sup> and interpreted either as a two-step (electron capture followed by thermal emission), or as a single step (exchange) process.<sup>3</sup> It is doubtful, however, whether any of these models can be applied to the scattering of hot electrons at mK temperatures, given in particular the freeze-out of carrier emission from all, including the shallower ( $A^+/D^-$ ) bound states of the dopant species.<sup>4,5</sup> In the absence of free carrier screening at these temperatures, the long range nature of the Coulomb force makes the conventional model for charged impurity scattering as a succession of two-body encounters equally questionable.<sup>6</sup> (A similar situation arises in the physics of ionized gases, where the cumulative effect on a particle of the small deflections resulting from relatively distant encounters is more important than the effect of occasional large deflections from close encounters.<sup>7</sup>) We tackle these issues by resorting to a statistical model for charged impurity scattering which is free from these limitations. We consider a random distribution of positively and negatively charged centers in equal densities  $N_{scatt}$  (a free parameter in the model), so that the space-charge density averages to zero on a scale of distances large compared with the mean spacing of the scattering centers. The latter contribute thus a microscopic, spatially fluctuating term to the collection field. Assuming the positive and negative centers to be spatially uncorrelated, this contribution is described statistically by the Holtmark distribution,<sup>8-9†</sup> which we sample out at the successive time steps in the Monte Carlo simulation of electron motion.

† The mean value of the field in this distribution is  $\sim 10(q/4\pi\epsilon_0\epsilon_r)N_{scatt}^{2/3}$ , which gives 1 V/cm for  $N_{scatt} \sim 4 \times 10^{10} \text{ cm}^{-3}$ .

## A. Broniatowski

We apply Nathan's model for hot electron transport in germanium<sup>10</sup> in order to obtain the electron velocity at each time step in the simulation as a function of the electric field. This model will be valid on the condition that phonon scattering be isotropic, and that the intervalley scattering time be long compared to the intravalley scattering time so that the energy distribution of the electrons in each valley is determined only by intravalley scattering.<sup>†</sup> A closed expression then obtains for the drift velocity  $\mathbf{v}_i$  of an electron in the  $i$ th valley as a function of the field  $\mathbf{E}$ . A single set of experimental data is needed in order to determine this dependence explicitly, namely the electron velocity-versus-field relationship along the  $\langle 100 \rangle$  symmetry axis.<sup>10,11</sup>

Whether an intervalley transition occurs or not in the time interval between successive steps is decided by the pass/fail test of the latter process, a function of the intervalley transition rate. In this respect, the hypotheses of Nathan's model imply that the probability per unit time  $\nu_i$  for an electron to scatter out of the  $i$ th valley is a function of the field through the single parameter  $E_{eff,i} = |\boldsymbol{\gamma}_i^{1/2} \cdot \mathbf{E}|$ , where  $\boldsymbol{\gamma}_i$  is the reciprocal effective mass tensor for the valley under consideration.<sup>12</sup> We derive the  $\nu(E_{eff})$  relationship directly from the fit of simulated charge collection patterns to the patterns obtained experimentally.<sup>13</sup>

The anisotropy of hole velocities is on a lesser scale compared with electrons, not exceeding  $\sim 20\%$  between the  $\langle 100 \rangle$  and the  $\langle 111 \rangle$  field orientations (at 8K).<sup>14</sup> As an approximation, we neglect the hole anisotropy altogether, and apply to all field orientations the same velocity-versus-field relationship, as determined in the  $\langle 100 \rangle$  direction of the field.<sup>11</sup>

### 3. SIMULATION CODE FOR CHARGE COLLECTION

Based on this model for carrier transport, we have developed a computation code for charge collection and signal simulation in the Edelweiss dark matter detectors.<sup>15</sup> The calculation is in three stages: Stage (1) solves Laplace equation for the electrostatic potential in the given biasing conditions of the detector, and for the weighing potential pertaining to each set of collection electrodes. Stage (2) generates a cloud of electrons and holes at the site of energy deposition, in a spherical volume of a size comparable to the range of a photoelectron ( $\sim 10\ \mu\text{m}$  for a 60 keV energy deposit). Electrons are assumed to be equally distributed initially among the four energy valleys. Limitation in computing power requires that the carriers

<sup>†</sup> An additional condition for the present case is that the field should not vary by a large amount over a range of distances comparable to the electron velocity times the intravalley scattering time.

### Carrier anisotropy in Ge at mK temperatures: modeling

of each type should be bunched into a number of charge packets, a few hundred typically. Stage (3) calculates the trajectories of the charge packets and the time dependence of the detector signals using Ramo's theorem,<sup>16</sup> with a time step of a nanosecond typically. Carriers reaching a free surface of the crystal are considered trapped. Specific features of the code include the ability to impose an arbitrary orientation of the device relative to the crystal axes, so that anisotropy effects in charge collection can be modeled in a wide range of situations.

#### 4. SIMULATED CHARGE COLLECTION PATTERNS AND COMPARISON TO EXPERIMENT

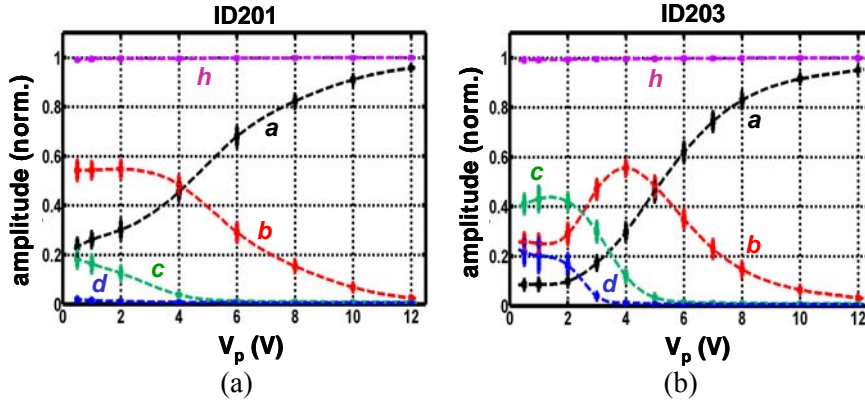


Fig. 2. Best fit simulations of the charge collection patterns for devices ID201 (a) and ID203 (b), respectively. Both devices are fitted with six charge measurement channels (*a*, *b*, *c*, *d*, *g* and *h* respectively), as described in fig. 1 of ref. 1. Simulations of the charge signals in the different channels are for 60 keV photon interactions, the sites of energy deposition being along the detector axis, and distributed in depth from the bottom surface of the crystal in accordance with the absorption profile for photons of that energy. Data for each value of the detector bias ( $V_p$ ) correspond to  $\sim 200$  simulated events. The signal amplitudes are normalized to unity for full charge collection in the *h* channel. The dashed lines are guide for the eyes only. The error bars represent the standard deviation of the (60 keV) simulated signal amplitudes about the mean.

Figures 2 (a) and (b) represent best fit simulations of the electron collection patterns recorded experimentally (figs. 2 (a) and (b) of ref. 1). The values obtained for  $N_{scatt}$  are  $5.0 \times 10^{10} \text{ cm}^{-3}$  for device ID201 and  $1.5 \times 10^{10}$

### A. Broniatowski

$\text{cm}^{-3}$  for ID203, respectively. These values are considered accurate to  $\pm 20\%$ , as a variation in  $N_{scatt}$  by that amount alters significantly the quality of the fits, at the lower detector biases especially ( $V_p < \sim 5$  V). Consistent with experiment, variations in  $N_{scatt}$  have little incidence on the collection patterns at the higher values of the detector biases ( $V_p > \sim 8$  V). Slight differences are observed at the lower detector biases in the simulated compared to the experimental data for the ‘ $h$ ’ channel amplitude (which records the net amount of carrier trapping in the device). These differences are explained by the neglect of bulk carrier trapping in the simulations.

## 5. DISCUSSION

This paper presents a new model for carrier scattering by Coulomb centers in germanium, based on a statistical treatment of the field fluctuations they produce on the microscopic scale, and appropriate for the temperature range of carrier freeze-out (below 1 K typically). The model reproduces quantitatively the charge collection patterns obtained with cryogenic Ge detectors operated in a wide range of biasing conditions, and also the time structure of the charge collection signals.<sup>13</sup>

The surprise comes from the densities of the scattering centers obtained from the analysis of our experimental data. The values obtained for  $N_{scatt}$  are  $1.5 \times 10^{10} \text{ cm}^{-3}$  for device ID203 ( $n$ -type, doped to  $10^{11} \text{ cm}^{-3}$ ), and  $5 \times 10^{10} \text{ cm}^{-3}$  for device ID201 (ultra-pure Ge,  $n$ -type with  $N_d - N_a < 10^{10} \text{ cm}^{-3}$ ). (Let us remind that  $N_{scatt}$  is the density of scattering centers of one sign only, so that the overall density of scatterers is twice that number.) Especially noteworthy is the fact that the strength of impurity scattering is reversed from the known concentration of dopant impurities in the crystals, as the crystal with the higher dopant concentration shows lower scattering at low field than the one with the lower concentration. The scattering center densities for both devices also exceed by orders of magnitude the values obtained from thermally stimulated current measurements for the dopant-related (H-like) centers ( $\sim 10^7 \text{ cm}^{-3}$ )<sup>4,5</sup> in the same crystals at sub-kelvin temperatures. These facts altogether suggest that the scattering centers are *not* the dopant species, but deep level centers associated with still unidentified impurities or crystal defects. In view of these results, we believe that there is a need for a better characterization of the properties of the deep level trap centers in high-purity germanium at cryogenic temperatures, and of the related effects of carrier trapping and recombination under the operating conditions of the detectors.

## Carrier anisotropy in Ge at mK temperatures: modeling

### ACKNOWLEDGMENT

This study has been supported in part by Agence Nationale pour la Recherche under contract ANR-2010-BLAN-0422 02.

### REFERENCES

1. E. Olivieri et al., *J. Low Temp. Phys.* (2012). Proceedings LTD14. doi: 10.1007/s10909-012-0548-0.
2. B. Tell and G. Weinreich, *Phys. Rev.* **143**, 584 (1966).
3. P.J. Price and R.L. Hartman, *J. Phys. Chem. Solids* **25**, 567 (1964).
4. J. Domange et al., *J. Low Temp. Phys.* (2012). Proceedings LTD14. doi: 10.1007/s10909-012-0547-1.
5. E.M. Gershenzon et al., *Sov. Phys. Usp.* **23**, 684 (1980).
6. B.K. Ridley, *J. Phys. A* **10**, L79 (1977).
7. R.S. Cohen, L. Spitzer and P.M. Routly, *Phys. Rev.* **80**, 230 (1950).
8. J. Holtsmark, *Annalen der Physik* **58**, 577 (1919).
9. S. Chandrasekhar, *Rev. Mod. Phys.* **15**, 1 (1943).
10. M.I. Nathan, *Phys. Rev.* **130**, 2201 (1963).
11. J. Domange et al., *J. Low Temp. Phys.* (2012). Proceedings LTD14. doi: 10.1007/s10909-012-0535-5.
12. C. Herring and E. Vogt, *Phys. Rev.* **101**, 944 (1956).
13. A. Broniatowski, *paper in preparation*.
14. L. Reggiani et al., *Phys. Rev. B* **16**, 2781 (1977).
15. E. Armengaud et al., *Phys. Lett. B* **702**, 329 (2011) and references therein.
16. S. Ramo, *Proc. IRE* **27**, 584 (1939).